Glycerol-based Pressure Sensitive Adhesives: Synthesis and Applications

Fang-Yi Lin†, Benjamin Claypool‡, Michael J. Forrester†, Nacú Hernández†, Ashley Buss‡, Baker Kuehl†, and Eric W. Cochran†*

†Department of Chemical and Biological Engineering, Iowa State University, Ames, IA 50011, United States

‡Department of Civil, Construction and Environmental Engineering, Iowa State University, Ames, IA 50011, United States

E-mail: ecochran@iastate.edu

Abstract

Block copolymers derived from glycerol, a cost-effective and plentiful resource, have demonstrated significant potential for pressure-sensitive adhesive (PSA) applications. This study focuses on functionalizing two monomers: acrylated glycerol and solketal acrylate, derived from glycerol, to synthesize two (meth)acrylate-based block copolymers, poly(methyl methacrylate-block-acrylated glycerol) (MMAAG) and poly(isobornyl acrylate-block-solketal acrylate-block-isobornyl acrylate) (IBASA), using reversible addition-fragmentation chain transfer (RAFT) polymerization. These elastomers, notable for their intrinsic tackiness, are formulated with plasticizers to achieve the desired PSA properties. We investigate their viscoelastic and morphological properties using dynamic shear rheology and small-angle X-ray scattering, respectively. The PSA performance is evaluated through 180° peel testing under various conditions, including different adherends, humidity levels, and peel rates. Our findings reveal that a benzoate ester-plasticized IBASA block copolymer, with a molecular weight of 100 kDa

and containing 20 wt% IBA, exhibits peel performance on par with 3M Scotch Magic Tape™. These results underscore the potential of glycerol-based PSAs as sustainable alternatives to traditional petroleum-based adhesives.

Keywords: Glycerol-based polymers, Pressure-sensitive adhesives, Sustainable materials, Green chemistry, Block copolymers.

Introduction

With a global push to diminish and ultimately cease our dependence on petroleum for both energy and materials, biodiesel and its byproducts, notably glycerol, have emerged as significant players. The production of biodiesel from various plant or animal sources not only yields fatty acid esters but also produces glycerol as a major byproduct, constituting approximately 10 wt% of the oil feed. This surplus of crude glycerol poses a financial challenge for the biodiesel industry, with production costs escalating by approximately $0.008 USD for every $0.01 USD decline in glycerol prices.[1–3] Given the substandard quality of crude glycerol, which necessitates costly refining for most potential applications, identifying new, value-added uses for this byproduct is imperative. Industrial applications that can accommodate the impurities present in crude glycerol are deemed particularly viable.

With appropriate functionalization, glycerol derivatives emerge as promising monomer candidates for polymerization, typically through substitution of glycerol with (meth)acrylic, vinylic, or allylic groups via (trans)esterification[4,5] or transvinylation.[6] These derivatives are compatible with various radical polymerization techniques,[7] though their multifunctional nature often designates them as crosslinkers. For example, Gogoi and Sarma developed a poly(glycerol acrylate) and curcumin crosslinked composite for chemical sensing.[8] Monofunctional monomers can be obtained by protecting the 2,3 hydroxyl groups of glycerol before introducing polymerizable functions, such as converting them to glycerol carbonate with phosgene or to ketal derivatives like solketal.[9] Poly(glycerol carbonate) has been utilized by Britz

et al. in lithium ion conductors,[10] while solketal, with its acid-sensitive ketal group, is notable in biomedical applications for its pH-responsive hydrolysis, facilitating the design of drug delivery systems. Solketal acrylate has been polymerized with hydrophilic macromonomers via atom transfer radical polymerization to create polymeric micelles for encapsulating hydrophobic drugs,[11–14] with their efficacy demonstrated by Jing *et al.* in cell viability tests with human breast cancer cells.[15] Furthermore, poly(glycerol mono(meth)acrylate)-based block copolymers, derived from hydrolyzing poly(soketal (meth)acrylate), have shown promise in creating stable magnetic fluids when combined with Fe_3O_4 nanoparticles.[16] While these applications underscore glycerol derivatives' value-added potential, their commercial implementation in high-value niches requires minimal volumes, making the source of raw materials negligible. Thus, the significant valorization of crude glycerin hinges on cost-effective and performance-advantaged applications capable of consuming large volumes to truly impact the market.

Globally, over 5 million tons of thermoplastic elastomers (TPEs) are consumed annually,[17] serving crucially in the development of pressure-sensitive adhesives (PSAs)—a market valued at US$10 billion in 2017, with a 6.4% annual growth rate worldwide.[18–20] PSAs adhere to surfaces under minimal pressure, such as finger pressure, without forming covalent bonds, yet resist peeling forces effectively. They are integral to various everyday products including labels, sticky notes, and tapes. Typically, PSAs comprise rubbers or TPEs, enhanced with tackifiers, plasticizers, and stabilizers. Predominantly, these formulations utilize petroleum-derived polymers like crosslinked acrylics, styrenic block copolymers, and silicones.[21] A PSA's efficacy hinges on its viscoelastic properties, evaluated through tack, peel, and shear assessments.[22] For optimal performance, a PSA must demonstrate liquid-like behavior at the application frequency (approximately 1 rad/s) to adequately wet and adhere to non-smooth surfaces upon contact.[23] High elastic and loss moduli (G' and G'') are essential at the debonding frequency (approximately 435 rad/s) for strong peel adhesion, indicating cohesive integrity.[24] Additionally, for effective creep resistance, PSAs should

maintain a robust elastic modulus in the terminal response regime ($\omega << 1$ rad/s). Formulating PSAs involves balancing these properties while considering resistance to UV radiation, humidity, and aging.

The transition towards renewable pressure-sensitive adhesives (PSAs) is a pivotal aspect of moving away from petroleum dependency. Derived predominantly from plant sources, bio-based PSAs leverage elastomers synthesized from plant oil derivatives, sugars, and starches. The inherent long aliphatic chains in these materials result in polymers with low glass transition temperatures (T_g) and desirable rubbery properties, making them suitable for PSA applications. Research has demonstrated the viability of using rubbery (co)polymers, derived from fatty acid esters[25–27] and soybean oil,[28–30] as PSAs once they have been cured. Innovatively, the incorporation of unsaturated vinyl groups from soybean oil with phosphorus groups enhances the flame retardancy of PSAs.[30] Emulating the structure of styrenic block copolymers, bio-based thermoplastic elastomers are developed into ABA-type block copolymers, where both the glassy and rubbery segments are derived from bio-based materials—for instance, glassy blocks from lactides,[31–33] γ-methyl-α-methylene-γ-butyrolactone from levulinic acid,[34] and isorsobide,[35] and rubbery blocks from ϵ-decalactone,[33] and menthide.[31,34] The formulation of PSAs also requires consideration of bio-based tackifiers and plasticizers, such as rosin esters and epoxidized soybean oil, respectively.[36,37] Lee *et al.* showcased a fully bio-based PSA system, including elastomer, tackifier, and plasticizer, demonstrating adhesive performance on par with commercial PSAs,[33] signifying a sustainable alternative in the adhesive industry.

Glycerol's role in pressure-sensitive adhesives (PSAs) has been traditionally confined to serving as a plasticizer, a limitation we aim to transcend in this study.[38] We present a green approach to synthesizing self-tackifying thermoplastic elastomers (TPEs) from glycerol, contributing to the development of new renewable PSA systems. We derive two monomers from glycerol: acrylated glycerol and solketal acrylate, which are subsequently polymerized with various glassy macromonomers via reversible addition-fragmentation chain transfer

(RAFT) polymerization. This process yields glycerol-based thermoplastic elastomers, including poly(methyl methacrylate-*b*-acrylated glycerol) diblock copolymers and poly(isobornyl acrylate-*b*-solketal acrylate-*b*-isobornyl acrylate) triblock copolymers, tailored for PSA applications. Owing to their inherent tackiness, these glycerol-based elastomers require only the addition of plasticizers through hot-melt blending to achieve desired adhesive properties. Their viscoelastic behavior is characterized by shear rheology, while their adhesive performance is assessed through 180° peel testing, considering variables such as adherend type, humidity level, and peel rate. Our findings underscore the potential of glycerol derivatives in PSA applications, showcasing their versatility beyond conventional uses.

Experimental

Materials

Glycerol (VWR), acrylic acid (Sigma-Aldrich), amberlyst 15 (Dow chemical), phenothiazine (Sigma-Aldrich), solketal (Sigma-Aldrich), methyl acrylate (Sigma-Aldrich), Novozym 435 (Sigma-Aldrich), 5Å Molecular sieve (Sigma-Aldrich), hydroquinone (Fisher), inhibitor remover (Sigma-Aldrich), S,S-dibenzyl trithiocarbonate (DBTTC, Sigma-Aldrich), methyl ethyl ketone (MEK, Fisher), dimethylformamide (DMF, Fisher), toluene (Fisher), and Benzoflex 2088 (Eastman) were used as received. Methyl methacrylate (Fisher), isobornyl acrylate (Sigma-Aldrich), and solketal acrylate were passed through the inhibitor remover column before conducting reactions. Both azobisisobutyronitrile (AIBN, Sigma-Aldrich) and , 1,1'-azobis(cyclohexanecarbonitrile) (ACHN, Sigma-Aldrich) were recrystallized from methanol. 2-cyanopropan-2-yl ethyl carbonotrithioate (CYCART) was synthesized based on the description elsewhere.[39]

Monomer syntheses

Acrylated glycerol (AG) was synthesized by reacting acrylic acid and glycerol through Fisher esterification. In a typical example, glycerol (500 g, 5.43 mol) and acrylic acid (520.36 g, 7.22 mol) were combined with the catalyst, amberlyst 15 (51 g, 5 wt%), in a reactor vessel. The reaction was carried out at 100 ^{o}C for 24 hr. The product was used as the monomer without further purification. ^{1}H NMR (400 MHz, DMSO): δ (ppm) = 3.27 - 4.25 (OCH_2CHCH_2O, 5H, m); 5.87 - 6.37 ($CH{=}CH_2$, 3H, m).

Solketal acrylate (SA) was synthesized through enzymatic transesterification of solketal and methyl acrylate adopted from Haring *et al.*[5] In a typical example, solketal (137.5 g, 1.04 mol) and methyl acrylate (358.33 g, 4.17 mol) were combined with an enzymatic catalyst, Novozym 435 (5.5 g, 4 wt% to solketal), in a reactor vessel. 5Å Molecular sieve (208.3 g, 1.5 w/w to solketal) was added to absorb the byproduct methanol. The reaction was carried out overnight at ambient temperature. The product was purified by filtration and dynamic distillation (yield: 76%). ^{1}H NMR (400 MHz, $CDCl_3$, TMS): δ (ppm) = 6.42, 6.13, and 5.82 ($CH{=}CH_2$, 3H, m); 4.32, 4.20, 4.15, 4.07, and 3.73 (OCH_2CHOCH_2O, 5H, m); 1.41 and 1.34 ($OC(CH_3)_2O$, 6H, m).

Synthesis of poly(methyl methacrylate-*block*-acrylated glycerol)

Poly(methyl methacrylate-block-acrylated glycerol) (MMAAG) block copolymer was adopted via two steps reversible addition-fragmentation chain transfer (RAFT) polymerization. The first step is the preparation of poly(methyl methacrylate) (PMMA) macromonomers with CYCART. For a typical synthesis, methyl methacrylate (50 g, 0.5 mol), CYCART (0.86 g, 4.5 mmol), AIBN (0.11 g, 675 μmol), and methyl ethyl ketone (50 g, 0.69 mol) were sealed and purged under argon for 30 min in a 250 mL round bottom flask. The reaction was carried out for 8 hr at 80 ^{o}C. The PMMA macro-CTA was crashed by methanol three times (from tetrahydrofuran solution) before further use. The second step is the chain extension of PMMA macromonomer with AG monomers. PMMA macro-CTA (14 g, 887 μmol), AG (150

g, 0.97 mol), ACHN (0.11 g, 443 umol), and dimethylformamide (DMF) (492 g, 6.74 mol) were sealed and purged under argon for 30 min in a 1 L round bottom flask. The reaction was carried out for 8 hr at 90 °C. The product was crashed by isopropanol three times (from DMF solution) and cryo-blended with 2 wt% phenothiazine before further processing.

Synthesis of poly(isobornyl acrylate-*block*-solketal acrylate-*block*-isobornyl acrylate)

Poly(isobornyl acrylate-block-solketal acrylate-block-isobornyl acrylate) (IBASA) was obtained via two steps RAFT polymerization. The first step is the preparation of poly(isobonyl acrylate) (PIBA) macromonomers with DBTTC. For a typical synthesis, isobornyl acrylate (18 g, 86 mmol), DBTTC (0.17 g, 600 μmol), AIBN (19.7 mg, 120 μmol) and toluene (18 g, 0.20 mol) were sealed and purged under argon for 30 mins in a 250 mL round bottom flask. The reaction was carried out at 80 °C for 8 hr. PIBA macromonomer was crashed by methanol three times (from tetrahydrofuran solution). The second step is the chain extension of PIBA macromonomer with SA monomers. PIBA macromonomer (14 g, 1.17 mmol), SA (200 g, 1.08 mol) , ACHN (0.14 g, 5.8 mmol) and toluene (214 g, 2.32 mol) were sealed and purged under argon for 30 mins in a 1 L round bottom flask. The reaction was carried out at 90 °C for 8 hr. The product was crashed by methanol three times (from tetrahydrofuran solution) before further processing.

Pressure sensitive adhesive formulation process

The pressure sensitive adhesives were prepared by hot-melt blending of the plasticizer with the block copolymer. Varying dosage of plasticizers were added at 100 - 120 °C for 30 min. The PSAs were then applied to thickness of 0.1 mm to a 2.54 cm polyethylene terephthalate (PET) film, with the help of draw down bar heated to 100 °C. After adhering specimens to stainless steel or glass adherends, the specimens were rolled twice by a 4.5 lb rubber wheel

at 12 in/min.

Peel testing specimens were prepared at varying humidity using saturated solutions.[40] The three humidity conditions were as follows: low humidity, 20-30% RH (potassium acetate); medium humidity, 40-60% RH (natural humidity); and high humidity, 80-90% RH (sodium chloride + wet rags). All specimens were conditioned for 24 hr before peel testing.

Characterization

^{1}H NMR spectra were recorded by a Varian MR-400 spectrometer (400 MHz). The molecular weight distribution was characterized by gel permeation chromatography (GPC) with an integrated Waters ACQUITY APC system equipped with Waters ACQUITY XT columns, a refractometry, and an UV spectrophotometer at dual wavelengths of 254 and 310 nm. The system is run in tetrahydrofuran at 1 mL/min at 50 °C. The system was calibrated by polystyrene standards. (Scientific Polymer Products Inc.) Samples were prepared at 5 mg/mL and passed through the 0.45 μm PTFE filter before the acquisition.

Dynamic shear rheology was conducted on ARES-G2 Rheometer (TA instruments) under nitrogen atmosphere with 8 mm parallel plates. Temperature-dependent strain sweep was scanned to find the linear viscoelastic region (LVR), which is the range of strain showing constant modulus, of materials at different temperatures. The suitable strain values were obtained at frequency 1 rad/s under $\sim$ 0.2 N axial force. Subsequently, temperature-dependent frequency sweep was performed in between 1 and 100 rad/s under ca. 0.2 N axial force within the LVR of the material. Time-temperature superposition (TTS)[41] was applied to generate the master curve for each material. Isochronal testing, which is the temperature sweep at constant strain and frequency, was conducted with a ramp rate of 10 °C/min under ca. 0.2 axial force and a suitable strain within the LVR of the material at 40 °C.

Small angle X-ray diffraction (SAXS) measurements were performed using a XENOCS Xeuss 2.0 SWAXS system 30W microfocus with monochromatized X-ray wavelength of λ = 1.54189 Å from Cu $\kappa\alpha$ radiation. Data were collected by Pilatus 1M detector at a sample-

to-detector distance of 2514 mm calibrated by a silver behenate standard. he corresponding scattering vector (q) window is 0.004 - 0.2 $Å^{-1}$. Data was collected at room temperature in vacuum with 10 mins exposure. Samples were annealed for 24 hrs at 50 °C above the highest T_g block.

Adhesive performance analysis

The adhesive performance was determined via 180° peel testing using the I-MASS SP-2100 slip-peel tester. The peel rate was 30.5 cm/min if not specified. Initial delays of two seconds followed by a 20 second test duration was used. The results were analyzed by the statistical software JMP using analysis of variance (ANOVA) tests. Tukey's HSD, with $\alpha = 0.05$, was used when comparing the means to determine statistically significant differences.

Results and Discussion

Synthesis and rheology of MMAAG block copolymer

Poly(methyl methacrylate-block-acrylated glycerol) (MMAAG) block copolymers are synthesized as outlined in Figure 1a. During monomer preparation, an excess of acrylic acid facilitates Fisher esterification, enhancing the functionality of AG to slightly above one (1.2) as confirmed by NMR results depicted in Figure 1a. The AG reaction mixture proceeds directly to chain extension with PMMA (number-average molecular weight M_n = 39, 150 Da, dispersity $Đ$=1.25, and mass yield = 99%). To optimize the balance between tackiness and mechanical integrity, the PMMA content is kept below 20% during chain extension. The resulting MMAAG block copolymer yields a mass composition of 21% with an overall yield of 54%, corresponding to a bio-based content of >50%. The composition is determined by weight due to the overlap of methoxy signals from PMMA (δ 3.43) with those of glycerol esters (δ 3.20 - 4.37) in the ^{1}H NMR spectrum, as illustrated in Figure 1a. Polymerization branching results in a block copolymer with M_n = 1, 007, 200 Da and $Đ$=2.18, with molecular

weight distribution curves presented in Figure S1. The broader distribution and less than standard peak shape is a consequence of the multifunctional nature of the monomer.

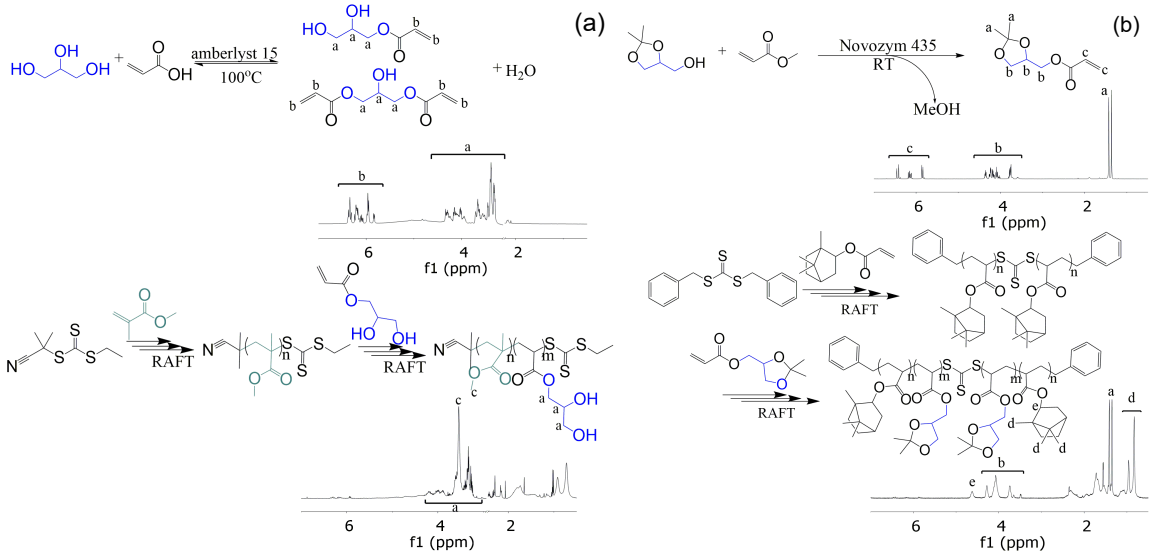

Figure 1: (a) Scheme of **MMAAG** preparation and the corresponding ^{1}H NMR spectra. (b) **IBASA** preparation and the corresponding ^{1}H NMR spectra

Post-synthesis, the **MMAAG** block copolymer's dynamic shear rheology was assessed, with the master and isochronal curves displayed in Figure 2. The shear modulus of **MMAAG** spans from 10^3 to 10^5 Pa across the application frequency range of 10^{-2} to 10^2 rad/s (Figure 2a, aligning with the Dahlquist criterion for effective PSAs, which mandates a G' under $33,000$ Pa at application temperature.[42] AG's plentiful hydroxyl groups enhance adhesion, particularly on hydrophilic interfaces like stainless steel and glass, due to their functional tackiness.[43] Yet, Figure 2b shows an isochronal curve where G' and G'' start to increase at 130 $°C$, signaling potential uncontrolled curing at elevated temperatures and is the result of esterification, transesterification and alkene polymerization reactions. This observation is further supported by the absence of a distinct entanglement plateau in the medium frequency range within the master curve (Figure 2a), but the emergence of an additional plateau indicating time-temperature superposition (TTS) failure at lower frequencies. Such behavior points to changes in polymer architecture and mechanical properties due to curing, driven by radical propagation through AG's multi-functional pendent vinyl groups. Despite the addi-

tion of the radical inhibitor phenothiazine, curing occurs, suggesting that **MMAAG** might not be compatible with the proposed hot-melt blending process for PSA formulation. This method, a prevalent manufacturing technique for PSAs, involves melding elastomers with additives and applying the blend onto backing films in their melted state. The increase in **MMAAG**'s shear modulus at high temperatures could compromise its tackiness and hinder processing performance.

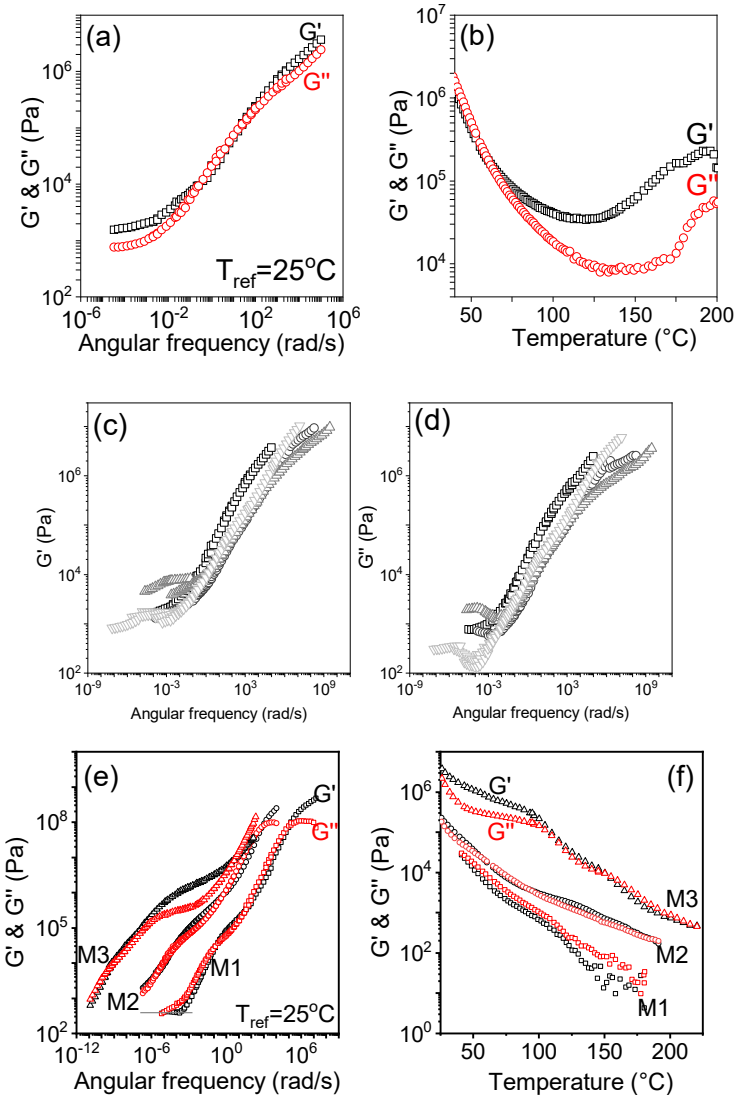

Figure 2: (a) Master curves and (b) isochronal curve of MMAAG block copolymer. (c) G' and (d) G" Master curves of □ **MMAAG** ∘ **MMAAG1** △ **MMAAG2** ▽ **MMAAG3** at reference temperature of 25 °C. (e) master curve and (f) isochronal curve of **M1** □, **M2** ∘, and **M3** △.

MMAAG-based PSA formulations

Table 1: MMAAG-based PSA formulation

Entry	Plasticizer[a]	Avg. peel force ($N/2.54cm$)
MMAAG1	Benzoflex 2088	1.03
MMAAG2	Tributyl citrate	0.33
MMAAG3	Triethyl citrate	0.23

a The plasticizer loading is 30 wt% to MMAAG.

Owing to their inherent self-tackiness, the PSA formulation of **MMAAG** omits tackifiers, incorporating only plasticizers to lower production costs. The plasticizers utilized are detailed in Table 1. Benzoflex 2088 (Eastman, Inc.), a benzoate ester-based commodity plasticizer and two citric acid derived ester plasticizers were chosen. We advocate for the eco-friendlier hot-melt blending process for PSA production, which necessitates only heat, eliminating the need for solvent assistance. Following formulation, MMAAG-based PSAs were subjected to dynamic shear rheology characterization and 180^o peel testing, with master curves displayed in Figure 2c-d. Post-plasticization, PSAs exhibit a 20-40% reduction in shear modulus across the $1 - 100$ rad/s range. Notably, **MMAAG2** and **MMAAG3** show a higher shear modulus at lower frequencies (< 0.01 rad/s), suggesting more pronounced crosslinking compared to **MMAAG1**, whose lower degree of crosslinking likely contributes to its enhanced tackiness, as supported by the highest average peel force among the three PSAs, detailed in Table 1. Consequently, Benzoflex 2088 was selected for subsequent glycerol-based PSA formulations. Due to the thermal crosslinking instability of pure **MMAAG** and its PSAs, alternative synthesis methods for glycerol-based PSAs with improved thermal crosslinking stability for hot-melt applications were explored; however, the potential of **MMAAG** elastomers in PSA applications remains promising, particularly if considering solvent blending, and could be extended beyond the confines of this study. It's worth noting that all three PSAs demonstrated cohesive failure during peel tests, indicating adhesive residue on both the adherend and PET film due to insufficient cohesive interac-

tion. Enhancing this interaction could involve modifying the block copolymer composition, increasing molecular weight, or altering its architecture, aspects considered in the design of future glycerol-based PSAs.

Synthesis and characterization of IBASA block copolymers

To enhance thermal crosslinking stability, boost cohesive strength and increase bio-content, IBASA block copolymers were designed and synthesized. The thermal crosslinking instability observed in **MMAAG**-based PSAs, primarily due to the multifunctional nature of AG monomers, prompted the strategy to confine glycerol-based monomers' functionality to unity. This entails limiting the functionalization to a single active hydroxyl group on glycerol, leading to the selection of solketal followed by transesterification with methyl acrylate. The synthesis of **IBASA**, a linear glycerol-based block copolymer, and its ^{1}H NMR spectra are illustrated in Figure 1b. This approach showcases two significant advantages of enzymatic transesterification over Fisher esterification: the lower polarity and easier removal of methanol, compared to water, and the acceleration of the reaction by Novozym 435, enabling near-complete conversion at room temperature. This method is environmentally benign, allowing for the recycling and reuse of both Novozym 435 and excess methyl acrylate, thus reducing energy consumption for both reaction and purification processes. The reaction's conversion rate hinges on the effective removal of methanol, achieved by employing a 5 Å molecular sieve. Subsequent dynamic distillation separates the excess methyl acrylate from solketal acrylate, streamlining the production process.

Further modifying the block copolymer architecture to enhance cohesive interactions, we transitioned from diblock to triblock copolymers, leveraging the telechelic chain transfer agent (CTA) DBTTC for the synthesis of solketal acrylate-based triblock copolymers via a two-step RAFT polymerization, as depicted in Figure 1b. DBTTC initiates the polymerization of isobornyl acrylate monomers to form PIBA macromonomers. Isobornyl acrylate was selected for its high glass transition temperature within the acrylate family and sub-

stantial biomass content (approximately 75%),[44] leading to a block copolymer that contains over 60% bioderived content. The IBASA block copolymers, synthesized through PIBA macromonomers chain extended with SA monomers, are detailed in Table 2, with molecular weights and IBA block content varying across entries yet maintaining an overall copolymer molecular weight of 90-100 kDa. It is noted that **M3** may exhibit slight contamination from its PIBA macromonomers, as suggested by the discrepancy between IBA content and final molecular weight.

Table 2: Characteristics of IBASA block copolymers

Entry	Macromonomer M_n/Da ($Đ$)[a]	Block copolymer M_n/Da ($Đ$)[a]	IBA wt%[b]	Conv. %[b]	Mass yield%
M1	12 013 (1.29)	91 117 (1.35)	15	54	34
M2	27 379 (1.22)	92 750 (1.63)	21	77	61
M3	25 630 (1.20)	104 000 (1.72)	33	22	38

a Based on GPC results
b Based on ^{1}H NMR results

Rheological and morphological characterization of IBASA block copolymers

The rheological properties of IBASA block copolymers are depicted in Figure 2e-f. All IBASA copolymers exhibit moduli exceeding the Dahlquist criterion across the application frequency range, underscoring the necessity for plasticizers in the formulation process. A notable increase in shear modulus correlates with higher IBA content, with **M3** demonstrating significant disparity between G' and G'', indicative of robust cohesive interactions. The isochronal curves in Figure 2b confirm that IBASA copolymers remain uncured within the test range, affirming solketal acrylate's role in ameliorating the thermal crosslinking stability issues of glycerol-based copolymers. Notably, **M1** exhibits an additional low-frequency plateau at $G' = 300$ Pa in Figure 2b, potentially due to physical resistance from microstructures, with a plateau slope of 0.05, suggesting spherical microstructures.[45] Although **M2**

and **M3** do not display this microstructure plateau within the detectable range due to instrumental limitations, their low-frequency behavior parallels that of **M1**, suggesting similar creep resistance. These microstructures, believed to bolster mechanical strength, allow glassy blocks to act as physical crosslinks at application temperatures, enhancing the copolymers' suitability for PSA applications.

SAXS profile elucidate the morphology of IBASA and MMAAG block copolymers, as shown in Figure 3. In IBASA materials, a pronounced primary peak (q^*) signifies enhanced microphase separation for **M2** and **M3**, with the peak's intensity escalating alongside the IBA content. The morphology of **M1** presents complexity, warranting further discussion in subsequent sections. Domain spacing, calculated using $d = 2\pi/q^*$, stands at 52.4 nm for **M2**, 54.7 nm for **M3**, and 69.8 nm for **MMAAG**. The manifestation of higher-order peaks in SAXS profile facilitates morphology identification; for instance, the second peak in **M2** and **MMAAG** may suggest spherical microstructures in **M2** (peak ratio $1:\sqrt{2}$) and cylindrical microstructures in **MMAAG** (peak ratio $1{:}1.6 \approx 1:\sqrt{3}$). These peaks are somewhat broader than what would be expected for a well ordered microstructure and this is likely caused by two factors: meta-stable ordering and slight polymer branching. In the rheology isochronal sweep, we never observe the sharp peak that indicates an order-to-disorder transition, and thus the cause of the meta-stable structure. Additionally, the functionality of the solketal monomer is slightly higher than 1 due to some small amount of solketal hydrolysis and multi-acrylation, this branching will likely cause a broadening of these scattering peaks. The SAXS findings corroborate rheological data, revealing microstructures within IBASA block copolymers that are poised to enhance mechanical strength.

IBASA-based PSA formulation: the adherend and humidity effects

IBASA block copolymers were further formulated with Benzoflex 2088 plasticizer to create PSAs. These samples are denoted as **M***XY*, where X represents the IBASA batch and Y the weight percentage of Benzoflex 2088 incorporated. Comprehensive master curves of

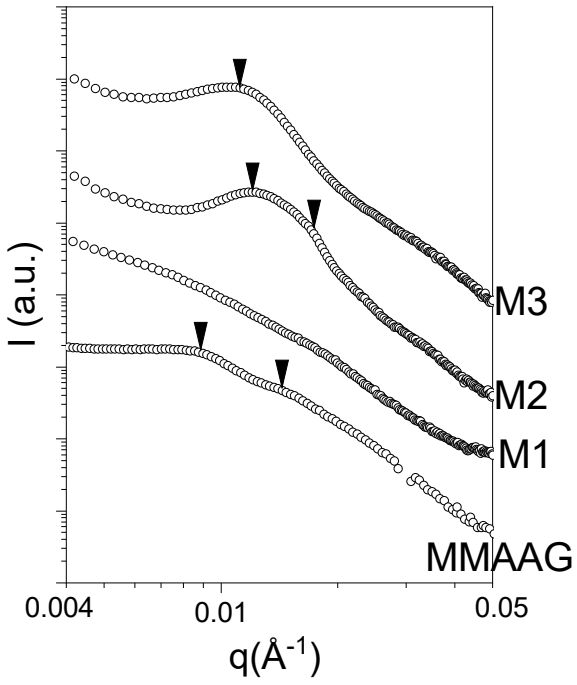

Figure 3: SAXS profile of IBASA and MMAAG block copolymers

the plasticized **M1** series, alongside their SAXS profile, are presented in Figures S2 and S3, respectively. Exhibiting thermal crosslinking stability, the hot-melt blended **M1** series PSAs demonstrate rheological profiles akin to **M1**. However, **M110** maintains a shear modulus comparable to **M1**, with a decrease observed as plasticizer content increases. The consistent modulus in **M110** might stem from the SAXS-observed enhancement in microphase separation, facilitated by Benzoflex 2088 blending, as indicated by a more pronounced primary peak at $q^* = 0.0115\text{Å}^{-1}$ with higher plasticizer dosages. This suggests that Benzoflex 2088's selective assimilation into IBA blocks strengthens segregation between the blocks, thus preserving the shear modulus of **M110** despite the plasticizer addition. This selective incorporation, improving mechanical integrity by isolating IBA from SA blocks, supports the comparable shear modulus between **M1** and **M110**, contrary to the anticipated reduction due to plasticization.

Figure 4a showcases the viscoelastic properties of the **M1** series PSAs within the fre-

quency spectrum typical of PSA applications, correlating these properties with tack and peel performance.[46] Specifically, $G'(\omega \sim 1\ rad/s)$ reflects the PSA's ability to adequately wet the adherend, establishing firm contact for superior tack performance. Conversely, both G' and G'' at $\omega \sim 435\ rad/s$ are indicative of the PSA's resistance to debonding, where a higher G' at this frequency typically signifies improved peel performance.[24] This relationship is evident in the peel adhesion trends of the **M1** series, where peel adhesion diminishes with an increase in plasticizer dosage, as depicted in Figure 4b. The reduction in modulus with added plasticizer, except for **M110** which maintains a modulus akin to **M1**, underscores the nuanced balance between tackiness and cohesive strength, crucial for optimal PSA performance.

While viscoelastic analyses offer insights into a PSA's inherent resistance to self-peeling, peel tests introduce practical considerations such as adherend type and relative humidity (RH). The moisture content within both the adhesive and adherend is known to impact adhesive bond strength significantly.[47] Despite the inherent hydrophobicity of IBASA block copolymers, our observations indicate that IBASA-based PSAs' adhesive performance is sensitive to variations in RH. Consequently, PSA samples were conditioned at three distinct RH levels for 24 hours before conducting peel tests. Figure 4b contrasts the peel adhesion of the **M1** series on glass and stainless steel under varying RH conditions. ANOVA analysis reveals that peel adhesion for IBASA-based PSAs does not significantly differ between the two types of adherends tested. However, RH levels markedly affect peel performance, with adhesion typically diminishing as RH increases, suggesting deteriorated bond integrity between the adherend and adhesive under higher humidity. Under these conditions, the **M1** series exhibits cohesive failure on both glass and stainless steel substrates. This failure mode, characterized by adhesive remnants on both the backing film and adherend, indicates inadequate cohesive strength within **M1** to prevent adhesive transfer. This observation underscores the necessity for enhancing cohesive interactions within the material to mitigate such transfer phenomena.

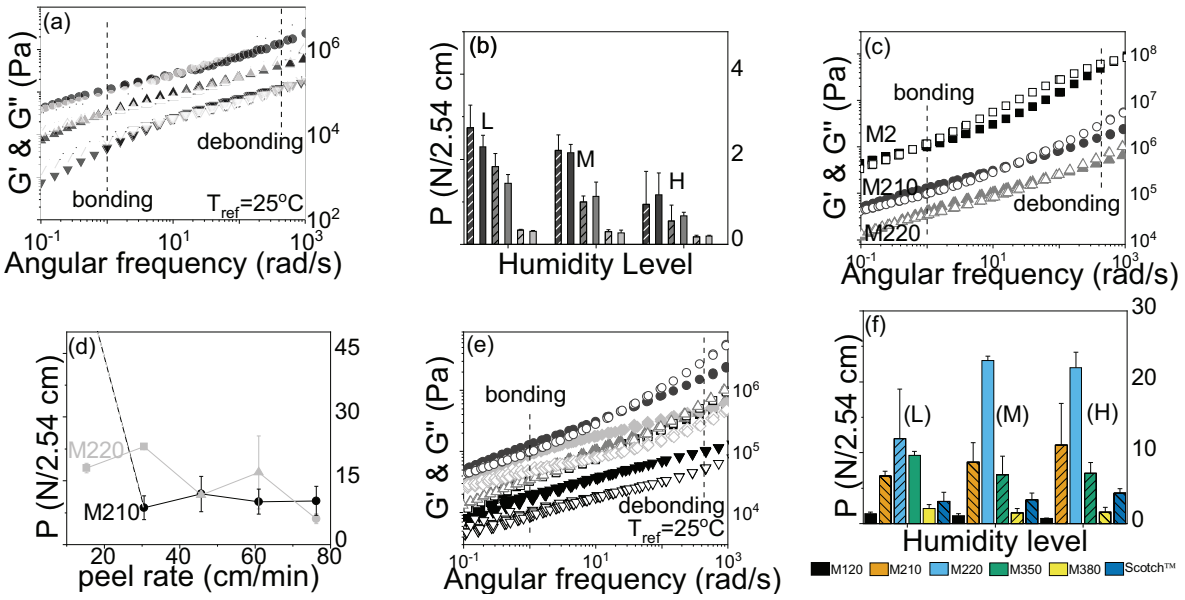

Figure 4: (a) The viscoelastic behavior within the application range with G' (filled) and G" (opened) and (b) peel adhesion on glass (stripped) and stainless steel (plain). For (a) and (b) the formulated PSAs from dark to light color are: **M110**, **M120**, **M140**. (c) The viscoelastic behavior within the application range with G' (filled) and G" (opened) and (d) peel adhesion conditioned at medium RH at different peel rate of **M2** series PSAs. The failure modes in (d) are ■ cohesive failure, • adhesive failure, and ▲ mixed failure. The peel adhesion of **M210** at the peel rate of 15.2 cm/min exceeds the instrument loading limit (50 N). (e) The viscoelastic behavior within the application range G' (filled) and G" (opened). PSAs from dark to light are **M120**, **M210**, **M220**, **M350**, and **M380**. (f) Peel adhesion at different humidity level of PSAs. L, M, and H correspond to low, medium, and high humidity level. The failure modes in (f) are □ cohesive failure, ▨ adhesive failure, and ▨ mixed failure.

The effect of peel rate on IBASA-based PSAs

The impact of peel rate on adhesion and failure mode complements the influences of adherend type and humidity, as the viscoelastic nature of PSAs aligns with frequency-dependent behaviors, a relationship underscored by various studies.[38,48] Under slow peeling, PSAs exhibit viscous flow characteristics, where adhesive deformation predominates, typically resulting in cohesive failure. Conversely, at higher peel rates, adhesives respond more elastically, enabling clean separation from the adherend, rendering peel adhesion rate-independent. At moderate peel rates, PSAs may exhibit a mix of cohesive and adhesive failures, leading to a complex adhesion behavior that might either continue to rise with peel rate or drop sharply

upon entering a predominantly adhesive failure domain. This variance in PSA response, contingent on peel rate, adherend type, and backing film, warrants further exploration. Figure 4c-d delineates the viscoelastic behavior and peel adhesion of the **M2** series PSAs, with their comprehensive master curves presented in Figure S4.

In Figure 4c, the **M2** series exhibits shear moduli exceeding 10^6 Pa, with values increasing as the IBA block content rises. Nonetheless, the presence of an entanglement plateau within the application frequency range signifies enhanced cohesive strength in the **M2** series PSAs. Following appropriate plasticization, the moduli of **M210** and **M220** adjust to within the optimal range for application. As depicted in Figure 4d, the introduction of plasticizer markedly influences the PSAs' response to varying peel rates. For **M210**, the peel adhesion transitions from exceeding the instrument's capability to stabilizing at approximately 10 $N/2.54$ cm, becoming relatively peel rate-independent, indicative of adhesive failure. This suggests a shift to mixed failure mode at 15 cm/min for **M210**. Conversely, the more heavily plasticized **M220** demonstrates a nuanced response; its softer nature amplifies its viscous characteristics compared to **M210**, predisposing it towards cohesive failure. Thus, the transition from cohesive to adhesive failure for **M220** occurs at a higher critical peel rate, with mixed failure observable at intermediate rates. These findings underscore the necessity for formulation adjustments to align the viscoelastic properties of PSAs with their intended application spectrum.

The effect of block copolymer composition on IBASA-based PSAs

Adjusting the peel adhesion of IBASA-based PSAs is feasible through modifying block copolymer compositions. Increasing the glassy IBA block content enhances material stiffness, necessitating higher doses of Benzoflex 2088 to satisfy the Dahlquist criterion for PSA formulation. For instance, the **M3** series PSAs incorporate 50 wt% or more Benzoflex 2088, with their rheological profiles presented in Figure S5. Dosages of plasticizer below 50 wt% result in uneven PSA spreading on the backing film. Even at higher dosages, as seen in

M350 and **M380**, the resultant PSA texture exhibits less homogeneity compared to the **M1** and **M2** series, emphasizing the influence of block composition and plasticizer content on the physical properties and application potential of IBASA-based PSAs.

To assess the influence of block copolymer composition on the peel performance of PSAs, we compared the peel adhesion of plasticized IBASA-based PSAs, as illustrated in Figure 4e, alongside their viscoelastic behavior within the application frequency range. The PSAs in comparison exhibit similar shear moduli, with **M210** slightly higher and **M380** marginally lower. ANOVA testing reveals significant impacts of block composition and relative humidity (RH) on peel adhesion. As shown in Figure 4f, the M2 series PSAs generally offer superior peel resistance, suggesting that a moderate IBA content optimally balances physical strength and energy dissipation capabilities. **M210** exhibits adhesive failure at low to medium humidity levels, with M2 series PSAs transitioning from adhesive to cohesive failure modes as humidity increases. Conversely, **M120** demonstrates weak peel adhesion with cohesive failure due to insufficient IBA content. Similarly, excessive IBA content in **M350** and **M380** diminishes peel adhesion, likely due to the high plasticizer dosages required for formulation. M3 series PSAs exhibit complex behavior across different humidity levels, transitioning from cohesive to adhesive failure. Future studies could explore the composition's effects on peel adhesion and failure modes more systematically, potentially incorporating tackifiers into **M3** series PSAs formulations. For reference, the peel adhesion of 3M Scotch™ Magic Tape, processed under identical humidity conditions, is also presented in Figure 4f. This comparison suggests that IBASA-based PSAs can match or outperform the commercial petroleum-based counterpart, 3M Scotch™ Magic Tape.

The evaluation of viscoelastic window

The master curve data informs the construction of the viscoelastic window depicted in Figure 5, framed by the G' and G'' values at 0.01 and 100 rad/s at the application temperature. Following Chang's methodology,[49] we employ the viscoelastic window concept to assess

potential PSA applications. MMAAG-based PSAs predominantly occupy the removable PSA domain, characterized by low modulus and dissipation, corroborated by their minimal peel adhesion observed in peel tests. Conversely, the viscoelastic window of IBASA-based PSAs spans from removable to high shear PSAs, contingent on the specific formulation. This variance suggests that IBASA-based PSAs, with their moderate modulus and energy dissipation capabilities, are primed for a broad spectrum of PSA applications.

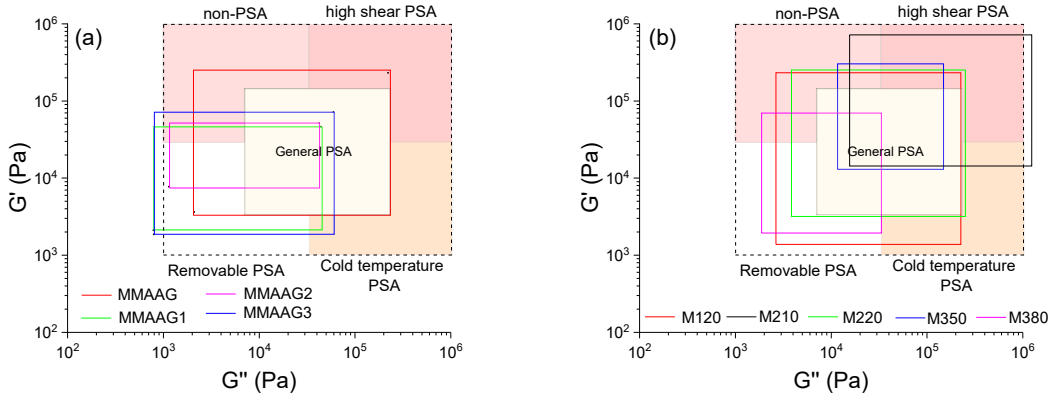

Figure 5: Viscoelastic window evaluation[49] for (a) MMAAG-based PSAs and (b) selected IBASA-based PSAs at 25 °C.

Conclusion

We synthesized glycerol-based block copolymers for pressure-sensitive adhesives (PSAs) via RAFT polymerization. Acrylated glycerol, with a functionality of 1.2, was polymerized with PMMA macromonomers, yielding MMAAG diblock polymers. Additionally, solketal acrylate—a glycerol derivative equipped with an acetal group to safeguard hydroxyl groups—underwent polymerization with PIBA macromonomers to produce linear IBASA block polymers. The formulation of PSAs involved hot-melt blending of these block copolymers with plasticizers, eliminating the need for additional tackifiers due to the materials' inherent tackiness. Both MMAAG and IBASA copolymers demonstrated microphase separation, as verified by dynamic shear rheology, with the glassy blocks acting as physical

crosslinks to fortify the PSAs' cohesive strength at their application temperature. Notably, MMAAG-based PSAs exhibited further curing and increased elasticity during the blending process, whereas IBASA-based PSAs showed superior thermal crosslinking stability up to 200°C, enhancing their peel adhesion as evidenced in peel tests. Comprehensive 180° peel tests assessed the performance of PSAs with various plasticizers, plasticizer loadings, adherends, and under different relative humidity conditions. Benzoflex 2088 emerged as the most effective plasticizer for these PSA formulations. Our statistical analysis indicated that peel adhesion of IBASA-based PSAs correlates with plasticizer loading and humidity level, independent of the adherend type. The content of the glassy block within the copolymers also significantly influenced the viscoelastic properties, impacting PSA formulation and peel performance. Formulations containing 20 wt% IBA and 10 wt% Benzoflex 2088 showcased superior peel performance, rivaling that of commercial 3M Scotch™ Magic Tape. This study posits that glycerol-based PSAs, particularly IBASA copolymers, span a broad application spectrum, from removable to high shear PSAs, showcasing the potential of these renewable materials to supplant conventional petroleum-based adhesives. While it will be necessary to improve some of the properties of this formulation, such as the cohesive strength, to achieve commercial readiness, the initial results are promising. Upon successful further formulation to enhance these properties, we would have a green PSA that meets all necessary criteria. This research introduces a novel platform utilizing abundant, cost-effective glycerol for creating renewable block copolymers, marking a significant stride towards sustainable adhesive technologies.

Acknowledgement

The authors thank the support by United States Department of Agriculture (USDA-NIFA-CAM 2014-38202-22318) and United Soybean Board (USB 1740-362-0710).

Supporting Information Available

GPC traces, master curves of **M1**, **M2**, and **M3** series PSAs, and SAXS profile of **M1** series PSAs.

References

(1) Anitha, M.; Kamarudin, S.; Kofli, N. The potential of glycerol as a value-added commodity. *Chemical Engineering Journal* **2016**, *295*, 119–130, DOI 10.1016/J.CEJ.2016.03.012.

(2) Haas, M. J.; McAloon, A. J.; Yee, W. C.; Foglia, T. A. A process model to estimate biodiesel production costs. *Bioresource Technology* **2006**, *97*, 671–678, DOI 10.1016/J.BIORTECH.2005.03.039.

(3) Quispe, C. A.; Coronado, C. J.; Carvalho Jr., J. A. Glycerol: Production, consumption, prices, characterization and new trends in combustion. *Renewable and Sustainable Energy Reviews* **2013**, *27*, 475–493, DOI 10.1016/J.RSER.2013.06.017.

(4) Wang, Y.; Aleiwi, B. A.; Wang, Q.; Kurosu, M. Selective Esterifications of Primary Alcohols in a Water-Containing Solvent. *Organic Letters* **2012**, *14*, 4910–4913, DOI 10.1021/ol3022337.

(5) Haring, D.; Wagner, E.; Bruchmann, B.; Beck, E.; Hauer, B. Enzymatic production of (meth)acrylic acid esters. **2006**, *1*, US patent 0141593 A1, DOI US␣20100322867A1.

(6) Pichavant, L.; Guillermain, C.; Coqueret, X. Reactivity of Vinyl Ethers and Vinyl Ribosides in UV-Initiated Free Radical Copolymerization with Acceptor Monomers. *Biomacromolecules* **2010**, *11*, 2415–2421, DOI 10.1021/bm1005883.

(7) Pham, P. D.; Monge, S.; Lapinte, V.; Raoul, Y.; Robin, J. J. Various radical polymer-

izations of glycerol-based monomers. *European Journal of Lipid Science and Technology* **2013**, *115*, 28–40, DOI 10.1002/ejlt.201200202.

(8) Gogoi, B.; Sarma, N. S. Poly-glycerol acrylate and curcumin composite: its dual emission fluorescence quenching and electrical properties for sensing 2-vinyl pyridine. *Journal of Materials Science* **2015**, *50*, 7647–7659, DOI 10.1007/s10853-015-9329-x.

(9) Kenar, J. A.; Knothe, G. 1,2-isopropylidene glycerol carbonate: Preparation, characterization, and hydrolysis. *JAOCS, Journal of the American Oil Chemists' Society* **2008**, *85*, 365–372, DOI 10.1007/s11746-008-1201-6.

(10) Britz, J.; Meyer, W. H.; Wegner, G. Blends of Poly(meth)acrylates with 2-Oxo-(1,3)dioxolane Side Chains and Lithium Salts as Lithium Ion Conductors. *Macromolecules* **2007**, *40*, 7558–7565, DOI 10.1021/MA0714619.

(11) Qui, X.; Liu, G.; Qiu, X.; Liu, G. Water-dispersible fluorescent nanospheres from poly(solketal acrylate)-block-poly(2-hydroxyethyl acrylate). *Polymer* **2004**, *45*, 7203–7211, DOI 10.1016/J.POLYMER.2004.08.035.

(12) Zhen, Y.; Wan, S.; Liu, Y.; Yan, H.; Shi, R.; Wang, C. Atom Transfer Radical Polymerization of Solketal Acrylate Using Cyclohexanone as the Solvent. *Macromolecular Chemistry and Physics* **2005**, *206*, 607–612, DOI 10.1002/macp.200400414.

(13) Tang, X.; Pan, C. Double hydrophilic block copolymers PEO- b -PGA: Synthesis, application as potential drug carrier and drug release via pH-sensitive linkage. *Journal of Biomedical Materials Research Part A* **2008**, *86A*, 428–438, DOI 10.1002/jbm.a.31515.

(14) Zhang, D.; Zhang, H.; Nie, J.; Yang, J. Synthesis and self-assembly behavior of pH-responsive amphiphilic copolymers containing ketal functional groups. *Polymer International* **2010**, *59*, 967–974, DOI 10.1002/pi.2814.

(15) Yang, J.; Zhang, D.; Jiang, S.; Yang, J.; Nie, J. Synthesis of Y-shaped poly(solketal acrylate)-containing block copolymers and study on the thermoresponsive behavior for micellar aggregates. *Journal of Colloid and Interface Science* **2010**, *352*, 405–414, DOI 10.1016/J.JCIS.2010.09.014.

(16) Wan, S.; Zheng, Y.; Liu, Y.; Yan, H.; Liu, K.; Zhang, Y.; Tsakalakos, T.; Muhammed, M. Fe3O4 Nanoparticles coated with homopolymers of glycerol mono(meth)acrylate and their block copolymers. *Journal of Materials Chemistry* **2005**, *15*, 3424, DOI 10.1039/b504607f.

(17) The Global Market for Thermoplastic Elastomers to Grow by 6.2% CAGR | Smithers. Date accessed: 2024-06-13; https://www.smithers.com/resources/2019/apr/global-market-for-thermoplastic-elastomers-to-grow.

(18) Pressure Sensitive Adhesives Market Size, Share & Forecast. Date accessed: 2024-06-13; https://www.alliedmarketresearch.com/pressure-sensitive-adhesives-market.

(19) Pressure Sensitive Adhesives Market Size | Global Industry Report 2024. Date accessed: 2024-06-13; https://www.grandviewresearch.com/industry-analysis/pressure-sensitive-adhesives-market.

(20) Sinha, B. Global Opportunity Analysis and Industry Forecast, 2017-2023. Date accessed: 2024-06-13; https://www.alliedmarketresearch.com/pressure-sensitive-adhesives-market.

(21) Creton, C. Pressure-Sensitive Adhesives : An Introductory Course. *MRS Bulletin* **2003**, *28*, 434–439, DOI 10.1557/mrs2003.124.

(22) Adams, R. D. *Adhesive bonding : science, technology and applications*; CRC Press, 2005; p 543.

(23) Creton, C.; Leibler, L. How does tack depend on time of contact and contact pressure? *Journal of Polymer Science, Part B: Polymer Physics* **1996**, *34*, 545–554, DOI 10.1002/(SICI)1099-0488(199602)34:3<545::AID-POLB13>3.0.CO;2-I.

(24) Yang, H. W. H. Water-Based Polymers As Pressure-Sensitive Adhesives-Viscoelastic Guidelines. *Journal of Applied Polymer Science* **1995**, *55*, 645–652, DOI 10.1002/app.1995.070550413.

(25) Vendamme, R.; Olaerts, K.; Gomes, M.; Degens, M.; Shigematsu, T.; Eevers, W. Interplay between viscoelastic and chemical tunings in fatty-acid-based polyester adhesives: Engineering biomass toward functionalized step-growth polymers and soft networks. *Biomacromolecules* **2012**, *13*, 1933–1944, DOI 10.1021/bm300523e.

(26) Li, A.; Li, K. Pressure-sensitive adhesives based on soybean fatty acids. *RSC Advances* **2014**, *4*, 21521–21530, DOI 10.1039/c4ra03557g.

(27) Wu, Y.; Li, A.; Li, K. Pressure Sensitive Adhesives Based on Oleic Acid. *Journal of the American Oil Chemists' Society* **2015**, *92*, 111–120, DOI 10.1007/s11746-014-2563-6.

(28) Li, Y.; Wang, D.; Sun, X. S.; Bardet, L.; Zu, S.; Vanoverloop, L.; Randall, D. Copolymers from epoxidized soybean oil and lactic acid oligomers for pressure-sensitive adhesives. *RSC Advances* **2015**, *5*, 27256–27265, DOI 10.1039/C5RA02075A.

(29) Ahn, B. K.; Sung, J.; Kim, N.; Kraft, S.; Sun, X. S. UV-curable pressure-sensitive adhesives derived from functionalized soybean oils and rosin ester. *Polymer International* **2013**, *62*, 1293–1301, DOI 10.1002/pi.4420.

(30) Wang, X. L.; Chen, L.; Wu, J. N.; Fu, T.; Wang, Y. Z. Flame-Retardant Pressure-Sensitive Adhesives Derived from Epoxidized Soybean Oil and Phosphorus-Containing Dicarboxylic Acids. *ACS Sustainable Chemistry and Engineering* **2017**, *5*, 3353–3361, DOI 10.1021/acssuschemeng.6b03201.

(31) Shin, J.; Martello, M. T.; Shrestha, M.; Wissinger, J. E.; Tolman, W. B.; Hillmyer, M. A. Pressure-sensitive adhesives from renewable triblock copolymers. *Macromolecules* **2011**, *44*, 87–94, DOI 10.1021/ma102216d.

(32) Zhang, J.; Severtson, S. J.; Lander, M. R. Pressure-sensitive adhesives having high bio-based content and macromonomers for preparing same. patent US 20150210907A1.

(33) Lee, S.; Lee, K.; Kim, Y. W.; Shin, J. Preparation and Characterization of a Renewable Pressure-Sensitive Adhesive System Derived from ϵ-Decalactone, L -Lactide, Epoxidized Soybean Oil, and Rosin Ester. *ACS Sustainable Chemistry and Engineering* **2015**, *3*, 2309–2320, DOI 10.1021/acssuschemeng.5b00580.

(34) Ding, K.; John, A.; Shin, J.; Lee, Y.; Quinn, T.; Tolman, W. B.; Hillmyer, M. A. High-Performance Pressure-Sensitive Adhesives from Renewable Triblock Copolymers. *Biomacromolecules* **2015**, *16*, 2537–2539, DOI 10.1021/acs.biomac.5b00754.

(35) Gallagher, J. J.; Hillmyer, M. A.; Reineke, T. M. Acrylic Triblock Copolymers Incorporating Isosorbide for Pressure Sensitive Adhesives. *ACS Sustainable Chemistry & Engineering* **2016**, *4*, 3379–3387, DOI 10.1021/acssuschemeng.6b00455.

(36) Cohen, E.; Binshtok, O.; Dotan, A.; Dodiuk, H. Prospective materials for biodegradable and/or biobased pressure-sensitive adhesives: A review. *Journal of Adhesion Science and Technology* **2013**, *27*, 1998–2013, DOI 10.1080/01694243.2012.696901.

(37) Vendamme, R.; Schuwer, N.; Eevers, W.; Schüwer, N.; Eevers, W. Recent synthetic approaches and emerging bio-inspired strategies for the development of sustainable pressure-sensitive adhesives derived from renewable building blocks. *Journal of Applied Polymer Science* **2014**, *131*, 40669, DOI 10.1002/app.40669.

(38) Gardon, J. L. Peel adhesion. I. Some phenomenological aspects of the test. *Journal of Applied Polymer Science* **1963**, *7*, 625–641, DOI 10.1002/app.1963.070070219.

(39) Haven, J. J.; De Neve, J. A.; Junkers, T. Versatile Approach for the Synthesis of Sequence-Defined Monodisperse 18- and 20-mer Oligoacrylates. *ACS Macro Letters* **2017**, *6*, 743–747, DOI 10.1021/acsmacrolett.7b00430.

(40) Greenspan, L. Humidity fixed points of binary saturated aqueous solutions. *Journal of Research of the National Bureau of Standards-A. Physics and Chemistry* **1977**, *81A*, 89–96, DOI 10.6028/jres.081A.011.

(41) Dae Han, C.; Kim, J. K. On the use of time-temperature superposition in multicomponent/multiphase polymer systems. *Polymer* **1993**, *34*, 2533–2539, DOI 10.1016/0032-3861(93)90585-X.

(42) Silva, L. F. M. d.; Öchsner, A.; Adams, R. D. *Handbook of Adhesion Technology*; Springer Science & Business Media, pp 341–371, Google-Books-ID: CsKoeKzXvl8C.

(43) Wool, R.; Sun, X. S. *Bio-Based Polymers and Composites*; Elsevier, pp 149–201, Google-Books-ID: EubnllIloNwC.

(44) Voet, V. S.; Strating, T.; Schnelting, G. H.; Dijkstra, P.; Tietema, M.; Xu, J.; Woortman, A. J.; Loos, K.; Jager, J.; Folkersma, R. Biobased Acrylate Photocurable Resin Formulation for Stereolithography 3D Printing. *ACS Omega* **2018**, *3*, 1403–1408, DOI 10.1021/acsomega.7b01648.

(45) Kossuth, M. B.; Morse, D. C.; Bates, F. S. Viscoelastic behavior of cubic phases in block copolymer melts. *Journal of Rheology* **1999**, *43*, 167–196, DOI 10.1122/1.550981.

(46) Chang, E. P. Viscoelastic properties of pressure-sensitive adhesives. *Journal of Adhesion* **1997**, *60*, 233–248, DOI 10.1080/00218469708014421.

(47) Chang, T.; Sproat, E. A.; Lai, Y. H.; Shephard, N. E.; Dillard, D. A. A test method for accelerated humidity conditioning and estimation of adhesive bond durability. *Journal of Adhesion* **1997**, *60*, 153–162, DOI 10.1080/00218469708014416.

(48) Aubrey, D. W.; Welding, G. N.; Wong, T. Failure mechanisms in peeling of pressure-sensitive adhesive tape. *Journal of Applied Polymer Science* **1969**, *13*, 2193–2207, DOI 10.1002/app.1969.070131014.

(49) Chang, E. P. Viscoelastic Windows of Pressure-Sensitive Adhesives. *The Journal of Adhesion* **1991**, *34*, 189–200, DOI 10.1080/00218469108026513.

For Table of Contents Only

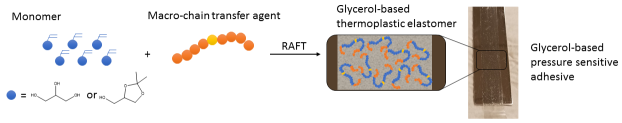

Synopsis: This work pioneers sustainable adhesives by transforming glycerol into high-performance pressure-sensitive adhesives.